Polyhedron 52 (2013) 1016–1023

Contents lists available at SciVerse ScienceDirect

Polyhedron

journal homepage: www.elsevier.com/locate/poly

Noble metal porphyrin derivatives bearing carboxylic groups: Synthesis, characterization and photophysical study

Christina Stangel [a], Dimitra Daphnomili [a], Theodore Lazarides [a], Marija Drev [b], Urša Opara Krašovec [b], Athanassios G. Coutsolelos [a,*]

[a] Chemistry Department, University of Crete, Voutes Campus, P.O. Box 2208, 71003 Heraklion, Crete, Greece
[b] Faculty of Electrical Engineering, University of Ljubljana, Tržaška c. 25, 1000 Ljubljana, Slovenia

ARTICLE INFO

Article history:
Available online 1 August 2012

Keywords:
Tetracarboxyporphyrins
Noble metals
X-ray studies
Photophysical studies
DSSCs

ABSTRACT

The synthesis and characterization of *meso*-carboxyphenylporphyrins metallated with transition metals Pt, Pd, Rh, and Ru are described. The photophysical properties of the dyes were investigated by UV–Vis absorption, emission spectroscopy and cyclic voltammetry. Structures of platinum and palladium derivatives were elucidated by X-ray. The activity of the formed complexes as dyes for DSSCs was studied, however the performance is rather low compared to the reference dye N719.

1. Introduction

Among the large number of synthetic porphyrin derivatives, the water-soluble ones are of particular interest due to their widespread applications that include sensitizers for DSSCs [1–5], in medicine and biology as drugs because of their capability to be enriched at the surface of a tumor allowing photodynamic therapy [6], as building blogs for crystal engineering [7] and supramolecular assemblies [3] and in catalysis [8,9]. Several porphyrins have been used as dyes, because of their strong absorption in UV–Vis region [10]. The most common being the free-base and zinc derivatives of the *meso*-benzoic acid substituted porphyrin TCPP. Grätzel et al. have reported efficient charge injection from the excited state of Zn-TCPP into the conduction band of TiO_2 ($IPCE_{Soret}$ = 42%), ($IPCE_{Qband}$ = 8–10%), however no AM1.5 normalized cell efficiencies were stated [11]. Photosensitization by Zn-TCPP, giving low solar-energy conversion efficiency (η = 1.1%) was reported from Boschloo and Goossens [12]. The best reported value (η = 3.5%) using TCPP as dye was achieved using deoxycholic acid (DCA) as a co-adsorbate and reported from Cherian and Wamser [2]. Monocaboxylate porphyrins with different metals were studied adsorbed on SnO_2 nanocrystalline semiconductor [13] with the Pd derivative being the one that gave the highest quantum yield of sensitized photocurrent generation. *Meso* or β-carboxy-derivatized porphyrins have been synthesized [14] with the position and nature of the bridge connecting the porphyrin ring and the carboxylic group having a significant influence on the photovoltaic properties of the sensitizers. More recently, Yella et al. introduced long alkoxyl groups into the porphyrin ring and achieved an unprecedented 12.3% energy conversion efficiency in combination with a cobalt-based electrolyte [15]. The long alkoxyl groups into this porphyrin ring reduce the dye aggregation. Reduction of η due to aggregation-induced energy transfer becomes a severe problem for porphyrin dyes because of their planar structural characteristics. Various Zn-metallated porphyrins have been tested as dyes for DSSCs, but few examples have been reported about metallated porphyrins with other metals like palladium, platinum for the same application. According to the literature, platinum porphyrins have not been tested as dyes in DSSCs but they have extensive applications into organic light emitting diodes (OLEDs). The most representative example is platinum (II) octaethylporphyrin (PtOEP) based OLEDs [16–18] in which quantum efficiency of the OLED achieved 6–7% photon/carrier. Shao and Yang have reported α new type of organic photovoltaic device by utilizing materials with long exciton lifetimes [19]. PtOEP was selected for the electron-donating material and C_{60} was used as the electron acceptor. Both possess strong triplet electron states, excellent thermal stability, and good ability to form thin films [19]. On the other hand, palladium porphyrins have applications

Abbreviations: Porphyrin 1, meso-tetra-[4-(4-ethoxy-4oxobutoxy)-phenyl]-porphyrin; N719 dye, di-tetrabutylammonium cis-bis(isothiocyanato)bis(2,2′-bipyridyl-4,4′-dicarboxylato)ruthenium(II); N3 dye, cis-bis(isothiocyanato)bis(2,2′-bipyridyl-4,4′-dicarboxylato ruthenium(II); AM 1.5, air mass = 1.5 (1000 Wm^{-2}); DSSC, dye-sensitized solar cell; FF, fil factor; I_{sc}, short-circuit current; ICPE, incident monochromatic photon-to-current conversion efficiency; V_{oc}, open circuit voltage; η, overall solar light energy conversion efficiency.

* Corresponding author.
E-mail address: coutsole@chemistry.uoc.gr (A.G. Coutsolelos).

0277-5387/$ - see front matter © 2012 Elsevier Ltd. All rights reserved.
http://dx.doi.org/10.1016/j.poly.2012.06.080

in thin films and in solid state solar cells. Kroeze and co-workers have reported bilayer semiconductor/antenna photovoltaic device structures, a smooth anatase TiO_2 film spin-coated with a carboxylated palladium porphyrin (PdTPPC) [20,21]. The charge separation efficiency was large and found to be 12% for the PdTPPC/TiO_2 bilayer. Ruthenium and rhodium metallated porphyrins are commonly used as catalysts in several catalytic reactions. The first use of metalloporphyrins bearing peripheral carboxylic groups has been reported in cross-coupling reactions [8] and in the hydrogenation of α,β unsaturated aldehydes [9]. As far as we know ruthenium carboxylate porphyrins have not been tested as dyes in DSSCs. A. Morandeira and co-workers reported the application in DSSCs of ruthenium phthalocyanine (Pc) axially coordinated with pyridyl carboxylic acid [22]. Therefore, since there are not many examples in the literature of porphyrin dyes metallated with noble metals studied as dyes in DSSC, we report herein the facile synthesis of various metallated porphyrins in high yields. Tetracarboxy porphyrins metaled with Pd, Pt, Rh, Ru and C_4 alkoxyl chains were synthesized for this purpose. Finally, their potential application as dyes for DSSCs was also studied.

2. Experimental

2.1. Materials and methods

All chemical were purchased from Aldrich chemical Co. and used without further purification. The NMR measurements were recorded on a Bruker AMX-500 or on a Bruker DPX-300. UV–Vis absorption spectra were measured on a Shimadzu MultiSpec-1501 spectrometer. HRMS was determined by a Bruker ultrafleXtreme MALDI–TOF spectrometer. Emission spectra were measured on a JASCO FP-6500 fluorescence spectrophotometer equipped with a red-sensitive WRE-343 photomultiplier tube (wavelength range: 200–850 nm). Quantum yields were determined from corrected emission spectra following the standard methods [23] using $[Ru(bpy)_3]Cl_2$ ($\Phi = 0.042$ in H_2O [24]) as standard. Emission lifetimes were determined by the time correlated single-photon counting technique using an Edinburgh Instruments mini-tau lifetime spectrophotometer equipped with an EPL 405 pulsed diode laser, at 406.0 nm with a pulse width of 71.52 ps and a pulse period of 200 ns, and a high speed red-sensitive photomultiplier tube (H5773-04) as detector.

2.2. X-ray crystal structure determination

Single crystals for **2c** and **2d** were obtained by slow evaporation of solvent of the complexes in 1:1(v/v) mixture of $CHCl_3$ and THF. The crystals were protected with paratone-N and mounted for data collection. X-ray diffraction data were recorded on STOE IPDSII diffractometer using graphite monochromated MoKα radiation ($\lambda = 0.71070$ Å). The data were collected at 140 K for **2c** complex and at 300 K for **2d**. Complete data set was collected using two ω scans with an increment of 1°, an exposure time of 2 min. for each oscillation and distance of 100 mm. Data reduction including absorption correction and cell dimension post refinement were performed using X-Area package software. The structure was solved using direct methods (*SHELXS-97*) and all non hydrogen atoms were refined with anisotropic displacement parameters using *SHELXL-97* [25] by full matrix least squares on F^2 values. All the hydrogen atoms were introduced at calculated positions as riding on bonded atoms.

2.3. Dye sensitized solar cells

All the chemicals for the TiO_2 paste preparation and other components of DSSC were used as received. Unique titanium oxide (TiO_2) sol–gel paste was deposited on the conduction glass electrode (TCO) using the "doctor blading" technique [26]. Layers were sintered at 450 °C for 1 h and later immersed in the ethanol solution of the porphyrin dyes for 12 h. For the counter electrode, 5 nm thick layer of platinum was sputtered onto a TCO glass substrate. The photoanode and the counter electrode were sealed together with a 25 μm thick polymer foil (Surlyn, DuPont) and the ionic liquid electrolyte containing 0.2 M I_2 was injected through the two holes predrilled into the counter electrode [27]. The average active area of the cells presented in this paper is 0.5 cm^2. The DSSCs characterization was performed with Keithley 238 source measure unit under the Oriel Class A sun simulator [28]. The level of standard irradiance (1000 W/m^2) was determined with a calibrated c-Si reference solar cell. The spectral response of the assembled DSSCs was analyzed with a Xenon lamp and a monochromator. The measurements were scanned in increments of 5 nm from 300 to 800 nm, while in order to obtain stable reading the 3 s delay was always applied between setting wavelength and measurement of the current.

2.4. Synthesis

Synthesis of porphyrin **1** and of complexes **2c** and **3c** were based on previously published procedures [8]. Hydrolysis of esters afforded the tetracarboxylic acid derivatives that were used for the DSSCs studies.

2.4.1. {Meso-tetra-[4-(4-ethoxy-4oxobutoxy)-phenyl]porphyrinato}-ruthenium(II)carbonyl (**2a**)

A mixture of porphyrin **1** (150 mg, 0.132 mmol), $Ru_3(CO)_{12}$ (150 mg, 0.235 mmol) and decalin (50 mL) was refluxed for 2 h under nitrogen atmosphere. The mixture was reduced to dryness under vacuum and the crude solid was dissolved in CH_2Cl_2 (40 mL) After washing with aqueous NaCl (2 × 30 mL) the organic layer was dried over Na_2SO_4, filtered and concentrated. The residue was purified by column chromatography on silica gel (CH_2Cl_2/EtOH, 100:0.3 v/v) to obtain **2a** as a dark red solid (158 mg, 95%). ^1H NMR (300 MHz, $CDCl_3$): $\delta = 8.74$ (s, 8H, Ar), 8.12 (dd, $J = 8.4$ Hz, $J = 2.1$ Hz, 4H, Ar), 8.01 (dd, $J = 8.3$ Hz, $J = 2.1$ Hz, 4H, Ar), 7.14 (m, 8H, Ar), 4.03 (m, 8H, CH2), 3.85 (m, 8H, CH_2), 2.24 (m, 8H, CH_2), 1.98 (m, 8H, CH_2), 1.15 (t, $J = 7.2$ Hz, 12H, CH_3) ppm. ^{13}C NMR (75 MHz, $CDCl_3$): $\delta = 181.9$ (Ru–*C*O), 173.2 (ester CO), 158.2, 144.3, 135.3, 135.1, 134.8, 131.6, 121.4, 112.6 and 112.4 (Ar*C* and porphyrin ring *C*), 66.8 (CH_2), 60.4 (CH_2), 30.5 (CH_2), 24.5 (CH_2), 14.0 (CH_3) ppm. UV–Vis: λ_{abs} (CH_2Cl_2) (ε, $mM^{-1}\,cm^{-1}$) 415 (97.7), 531 (10.1), 563 (5.6). HRMS-(MALDI-TOF): calc. for $[M–CO]^+$ $C_{68}H_{68}N_4O_{12}Ru$ 1234.3877, found 1234.3883.

2.4.2. {Meso-tetra-[4-(4-ethoxy-4oxobutoxy)-phenyl]-porphyrinato}-rhodium(III)chloride (**2b**)

Porphyrin **1** (150 mg, 0.132 mmol) was dissolved in benzonitrile (35 mL) under nitrogen atmosphere and refluxed for 5 min. $RhCl_3$ (55 mg, 0.26 mmol) was added and the solution was refluxed for additional 3 h, cooled, and reduced to dryness under vacuum. CH_2Cl_2 (40 mL) was added and the mixture was washed with aqueous NaCl (2 × 30 mL). The organic layer was dried over Na_2SO_4, filtered, concentrated, and the residue was purified by column chromatography on a silica gel (CH_2Cl_2/EtOH, 100:1 v/v) to obtain **2b** as a dark red solid (164 mg, 98%). ^1H NMR (500 MHz, $CDCl_3$): $\delta = 8.94$ (s, 8H, Ar), 8.17 (d, $J = 6.5$ Hz, 4H, Ar), 8.03 (d, $J = 7.0$ Hz, 4H, Ar), 7.27 (d, $J = 6.0$ Hz, 8H, Ar), 4.29 (m, 16H, CH2), 2.72 (t, $J = 7.5$ Hz, 8H, CH_2), 2.33 (q, $J = 6.5$ Hz, 8H, CH_2), 1.36 (t, $J = 7.0$ Hz, 12H, CH_3) ppm. ^{13}C NMR (75 MHz, $CDCl_3$): $\delta = 173.3$ (CO), 158.6, 142.1, 135.7, 135.0, 132.2, 120.5 and 112.6 (ArC and porphyrin ring C), 67.0 (CH_2), 60.5 (CH2), 29.9 (CH_2), 24.8(CH_2), 14.2 (CH_3) ppm. UV–Vis: λ_{abs} (CH_2Cl_2) (ε, $mM^{-1}\,cm^{-1}$) 427 (71.2), 537 (9.1), 574

(5.6). HRMS (MALDI-TOF): m/z calc. for $[M-Cl]^+$ $C_{68}H_{68}N_4O_{12}Rh$ 1236.3889, found 1236.3882.

*2.4.3. {Meso-tetra-[4-(4-ethoxy-4oxobutoxy)-phenyl]-porphyrinato}-platinum(II) (**2d**)*

$PtCl_2$ (175.7 mg, 0.660 mmol) was dissolved in benzonitle (30 mL) and refluxed for 1 h. Porphyrin **1** (150 mg, 0.132 mmol) was added and the solution was further refluxed for 1 h, cooled, and evaporated to dryness under reduced pressure. CH_2Cl_2 (40 mL) was added, and the mixture was washed with aqueous NaCl (2 × 30 mL). The organic layer was dried over Na_2SO_4, filtered, concentrated, and the residue was purified by column chromatography on a silica gel (CH_2Cl_2/EtOH, 100:0.3 v/v) to obtain **2d** as an orange solid (170 mg, 96%). ^{1}H NMR (300 MHz, $CDCl_3$): δ 8.78 (s,8H, Ar), 8.02 (d, J = 8.4 Hz, 8H, Ar), 7.20 (d, J = 8.57 Hz, 8H, Ar), 4.24 (m, 16H, CH_2), 2.67 (t, J = 7.2 Hz, 8H, CH_2), 2.28 (q, J = 6.9 Hz, 8H, CH_2), 1.35 (t, J = 7.2 Hz, 12H, CH_3). ^{13}C NMR (75 MHz,$CDCl_3$): δ 173.3 (CO), 158.6 (C), 141.1 (C), 134.8 (Ar), 134.7 (C), 133.8(Ar), 121.9 (C), 112.7 (Ar), 66.9 (CH_2), 60.5 (CH_2), 31.1 (CH_2), 24.8 (CH_2), 14.3 (CH_3). UV–Vis: λ_{abs} (CH_2Cl_2) (ε, $mM^{-1}\,cm^{-1}$) 406 (290.4), 512(25,4), 575 (4,9). HRMS (MALDI-TOF): m/z calc. for $C_{68}H_{68}N_4O_{12}Pt$ 1327.4481, found 1327.4475.

*2.4.4. General procedure for synthesis of porphyrins **3a**, **3b**, **3d***

To a solution of ester complex (**2a**, **2b** or **2c**, respectively) (0.0752 mmol) in THF/MeOH (10:6.4 v/v), aqueous 0.5 M KOH (73 mL) was added and stirred at room temperature for 24 h. The course of the reaction was monitored by T.L.C (CH_2Cl_2/MeOH 9:1 v/v). The solution was evaporated to dryness to afford the potassium salt as orange solid. The solid was dissolved in distilled water (100 mL), aqueous 2 N HCl was added dropwise until pH reached 3 and a precipitate was formed. It was filtered, washed several times with distilled water to afford a purple solid (yield 95%).

*2.4.4.1. {Meso-tetra-[4-(3-carboxypropoxy)-phenyl]-porphyrinato}ruthenium(II)carbonyl (**3a**).* ^{1}H NMR (300 MHz,DMSO-d_6): δ = 12.19 (br s, 4H, COOH), 8.60 (s, 8H, Ar), 8.08 (d, J = 7.8 Hz, 4H, Ar), 7.96 (d, J = 8.1 Hz, 4H, Ar), 7.32 (m, 8H, Ar), 4.28 (t, J = 6.0 Hz, 8H, CH_2), 2.56 (m, 8H, CH_2), 2.13 (t, J = 6.6 Hz, 8H, CH_2) ppm. ^{13}CNMR (75 MHz, DMSO-d_6): δ = 180.2 (Ru–*C*O), 174.2 (ester CO), 158.1, 143.4, 134.8, 133.9, 131.3, 121.1 and 112.6 (Ar*C* and porphyrin ring *C*), 66.8 (CH_2), 30.3 (CH_2), 24.5 (CH_2) ppm. UV–Vis: λ_{abs} (0.4% Et_3N in H_2O) (ε, $mM^{-1}\,cm^{-1}$) 413 (143.4), 533 (11.9), 569 (6.7) HRMS (MALDI-TOF): m/z calc. $C_{60}H_{52}N_4O_{12}Ru$ $[M-CO]^+$ 1122.2620, found 1122.2611.

*2.4.4.2. {Meso-tetra-[4-(3-carboxypropoxy)-phenyl]-porphyrinato}rhodium(III)chloride(**3b**).* ^{1}H NMR(300 MHz, DMSO-d6): δ = 12.21 (br s, 4H, COOH;, 8.93 (m, 8H, Ar), 8.14 (m, 8H, Ar), 7.41 (m,8H, Ar), 4.30 (m, 8H, CH_2), 2.56 (m, 8H, CH_2), 2.14 (m, 8H, CH_2) ppm. ^{13}C NMR (75 MHz, DMSO-d6): δ = 174.3 (CO), 158.4, 141.6, 134.9, 131.9121.1 and 112.9 (Ar*C* and porphyrin ring *C*), 66.5 (CH_2), 30.4 (CH_2), 24.5 (CH_2) ppm. UV–Vis: λ_{abs} (0.4% Et_3N in H_2O) (ε, $mM^{-1}\,cm^{-1}$) 422 (130.4), 535 (22.4), 572 (9.7). HRMS (MALDI-TOF): m/z calc. for $[M-Cl]^+$ $C_{60}H_{52}N_4O_{12}Rh$ 1123.2631, found 1123.2649.

*2.4.4.3. {Meso-tetra-[4-(3-carboxypropoxy)-phenyl]-porphyrinato}platinum(II) (**3d**).* ^{1}H NMR (300 MHz, CD_3SOCD_3): δ 8.76 (s, 8H, Ar), 8.02 (d, J = 7.2 Hz, 8H, Ar), 7.31 (d, J = 7.2 Hz, 8H, Ar), 4.24 (s br, 8H, CH_2), 2.50 (s br, 8H, CH_2), 2.12 (s br 8H, CH_2). ^{13}C NMR (75 MHz, CD_3SOCD_3): δ 174.6 (CO), 158.9 (C), 140.8 (C), 135.1 (Ar), 133.0 (C), 131.3 (Ar), 122.4 (C), 113.5 (Ar), 67.3 (CH_2), 30.7 (CH_2), 24.9 (CH_2) ppm. UV–Vis: λ_{abs} (0.4% Et_3N in H_2O) (ε, $mM^{-1}\,cm^{-1}$) 403 (141.4), 514 (15.8). HRMS (MALDI-TOF): m/z calc. for $C_{60}H_{52}N_4O_{12}Pt$ $[M]^+$: 1215.3229, found 1215.3235.

3. Results and discussion

3.1. Synthesis and characterization

The preparation of rhodium, ruthenium, palladium and platinum porphyrins with four anchoring groups is shown in Scheme 1. The free-base porphyrin **1** was prepared as previously described [8]. Insertion of rhodium, palladium and platinum was achieved by addition of $RhCl_3$, $PdCl_2$, $PtCl_2$ to porphyrin **1** in refluxing benzonitrile. Insertion of ruthenium was achieved by addition of $Ru_3(CO)_{12}$ to porphyrin **1** in refluxing decalin under N_2 atmosphere. The corresponding metal complexes **2a**, **2b**, **2c**, **2d** were obtained in high yields and were characterized by various spectroscopic techniques. UV–Vis absorption spectra of the formed metal-complexes are of normal type for five and four coordinated porphyrins (Table 1S). Indicative for the formation of the metal complexes is the blue or red shift for the Soret band related to the free base. In the case of Pd(II), Pt(II) and Ru(III) coordinated complexes the Soret band is blue shifted related to the free base (422 nm). On the contrary the Soret band of Rh(III) porphyrin is red-shifted (427 nm). Also the appearance of two Q bands for the metal porphyrins instead of four for the free base is characteristic for the metallation. In addition, the absence of negative chemical shift in the ^{1}H NMR spectra due to the hydrogen of pyrrole ring was indicative for the insertion of metal. The carboxylic acids derivatives were obtained by saponification using excess of KOH in THF/MeOH mixture followed by dropwise addition of 2 N HCl until formation of the precipitate. The UV–Vis absorption spectra of the carboxylic acids had the typical shift in the Soret band due to the solvent effect. In the carboxylic acid **3d**, the Soret band shifted at 403 nm and the Q-band at 514 nm.

3.2. Photophysical properties

It is known that Pt(II), Pd(II), Rh(III) complexes phosphoresce in the red region of the spectrum at both room temperature and 77 K and on passing from Pd(II) to Rh(III) and Pt(II) the effieciency of intersystem crossing to the first triplet excited state, following photoexcitation, increases due to enhancement of the heavy atom effect [29]. In our case the emission spectra of the metal tetraester porphyrinic complexes were measured at RT in air equilibrated dichloromethane solution and at 77 K in EtOH/MeOH glass. A collection of emission maxima, quantum yields and lifetimes are summarized in Table 1. Representative emission spectra are shown in Figs. 1 and 2. Compounds **2c** and **2d** were also studied by time resolved emission spectroscopy in dichloromethane at room temperature. The derivative **2c** shows the characteristic emission of palladium porphyrins with λ_{max} at 710 nm due to the phosphorescence and an emission at 510 and 616 nm due to the fluorescence at 298 K. The lifetime of the phosphorescence is 752 ns and that of the fluorescence is shorter than 1 ns. In a frozen glass at 77 K the emission spectrum shows small blue shift of the phosphorescence while no fluorescence was observed. The emission appears at 679 and 775 nm. The derivative **2d** exhibits only the characteristic phosphorescence of the platinum porphyrins with λ_{max} at 679 nm at 298 K. The lifetime of the phosphorescence is 585 ns. In a frozen glass at 77 K the phosphorescence has also been blue-shifted with emission maximum at 667 nm. In both **2c** and **2d** complexes the introduction of alkoxy chains is seen to slightly red shift the emission (5–10 nm) relative to their tetraphenyl analogs [30,31]. The observed lifetimes are considerably shorter than those observed in dearated solution of tetraphenyl poprhyrins. For the Rh derivative **2b** very weak fluorescence was observed [32] while phosphorescence is heavily quenched due to the presence of oxygen. As far as concerns Ru derivative **2a**, emission

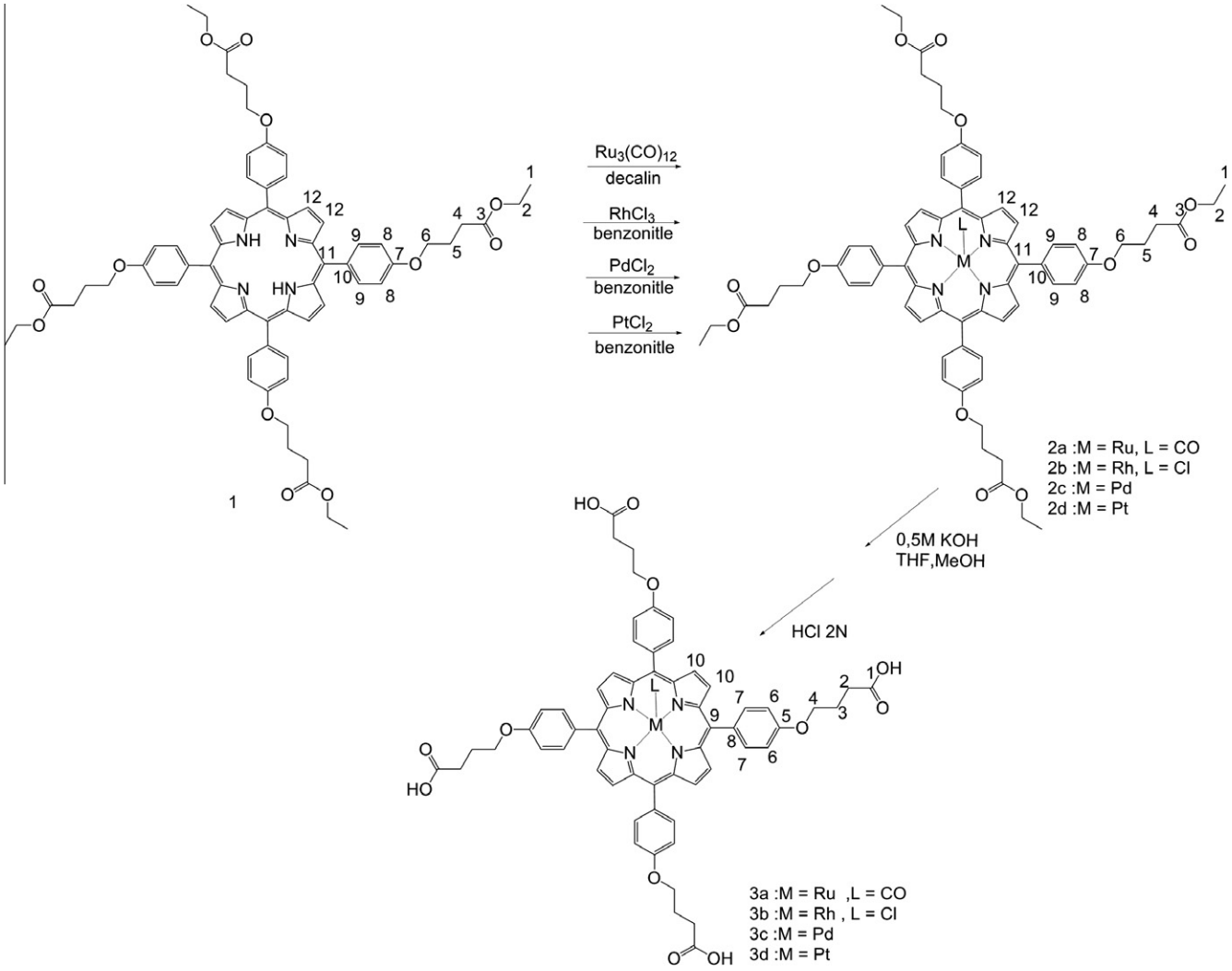

Scheme 1. Reaction scheme for complexes **2a–d** and **3a–d**.

Table 1
Summary of spectroscopic data for derivatives **2c** and **2d**.

Compound	Absorption	Emission			
	λ_{max}/nm (ε/M^{-1} cm^{-1})	λ_{max}/nm 298 K	Φ_{lum}[a] × 10^2 298 K	τ/ns 298 K	λ_{max}/nm 77 K
2c	420(402.3), 525(29.2), 559(3.5)	570, 616, 710[b]	1.110^{-3}[d] 1.9 10^{-2}[e]	<1, 752[f]	679, 775[g]
2d	406(290.4), 512(25.4), 475(4.9)	679, 746[c]	3.5	585	667,734

[a] Quantum yields were measured using $(Ru(bpy)_3)Cl_2$ in H_2O as the standard, as described in the experimental section.
[b] A band pass filter of 540 nm was used.
[c] A band pass filter of 600 nm was used.
[d] Fluorescence quantum yield.
[e] Phosphorescence quantum yield.
[f] A band pass filter of 600 nm was used for the detection of fluorescence with $\tau < 1$ ns, a band pass filter of 750 nm was used for the detection of phosphorescence with $\tau = 752$ ns.
[g] A band pass filter of 540 nm was used.

could not be detected, due to the presence of traces of unmetallated porphyrin [33,34] not detectable by the others spectroscopic methods.

3.3. Electrochemistry

The electrochemical properties of the metallated porphyrins were investigated by cyclic and square wave voltammetry in dichloromethane. The oxidation data are collected in Table 2. Usually, porphyrins show two-well defined reversible single-electron oxidations corresponding to ring oxidation and formation of the radical cation and dication [35]. In metalloporphyrins the ring or metal centered oxidations are determined by various factors such as the intrinsic redox potential of the porphyrinic ring, the metal center, the type of ligands on the metal and the properties of the solvent [36–38]. In tetraphenyl analog complexes it has been established that the first oxidation process involves porphyrin macrocycle oxidation. As has been reported electron withdrawing

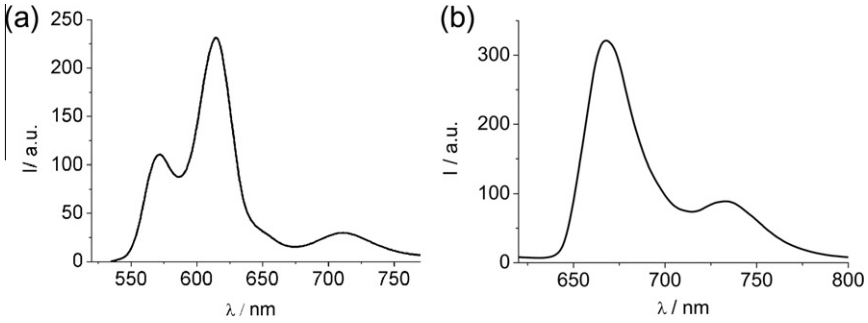

Fig. 1. Emission spectra in dichloromethane at room temperature of (a) **2c** and (b) **2d**.

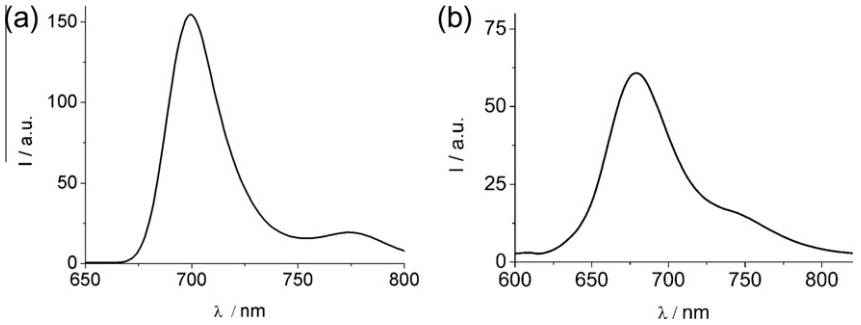

Fig. 2. Emission spectra in EtOH/MeOH (4:1, v/v) at 77 K of (a) **2c** and (b) **2d**.

Table 2
Oxidation and reduction data reported vs. Fc/Fc^+ in dichloromethane using tetrabutylammonium hexafluorophosphate ($TPAPF_6$) as supporting electrolyte. All data are reported vs the ferrocene/ferrocenium couple (Fc/Fc^+).

Compound	$E_{1/2}^{Ox1}$/V	$E_{1/2}^{Ox2}$/V	$E_{1/2}^{Red1}$/V
2a	0.29	0.72	–
2b	0.75	1.09	–
2c	0.55	0.95	−3.19
2d	0.64	1.01	−3.18

groups on para-position shifts the oxidations potentials to more positive values and electron donating groups shift the reduction potentials to more negative values with a linear Hammett relationship between the $E_{1/2}$ and the substituent constant σ [36]. Fig. 3 shows some representative cyclic voltammograms. All data are reported versus the ferrocene/ferrocenium couple (Fc/Fc^+). In our case, the oxidations are one-electron reversible. The complexes are more easily oxidized correlated to TPP analogs, which is evident of electron donating properties of the C_4-alkoxy chains to the porphyrin ring. The change in oxidation potential with different metal substitution follows the same order as that already reported [35] and for **2c** and **2d** are in the range 0.55–0.64 V and 0.95–1.01 versus (Fc/Fc^+). In CH_2Cl_2 only the first reduction potential was observed in the case of Pt and Pd complexes.

3.4. X-ray structure determination

Compound **2c** and **2d** were further ascertained by single crystal X-ray diffraction analysis (selected bond distances and angles are presented in Tables 2S and 3S). **2c** crystallizes in monoclinic system (Fig. 4). The structure is centrosymmetric and the asymmetric unit contains half of the porphyrin. The carbon atoms (C17–C22) lie in a plane $\mathbf{P_1}$ with an angle of 51.85 (0.19)° relative to the N4 plane and $\mathbf{P_2}$ (C11–C16) in a rather perpendicular position of an angle of 87.68 (0.30)°. The aliphatic chains were disordered and refined over two positions with occupation factors summing one. The isostructural Pt porphyrin crystallizes in orthorhombic system (Fig. 5). The data were collected at low temperature and the asymmetric unit contains half of the porphyrin ring. The plane of one phenyl ring forms an angle of 88.36 (0.30)° and the other of 48.18 (0.22)°. One of the ethoxy groups of the aliphatic chain were found disordered and refined over two positions with occupation factors summing one. In both structures the metals are on the

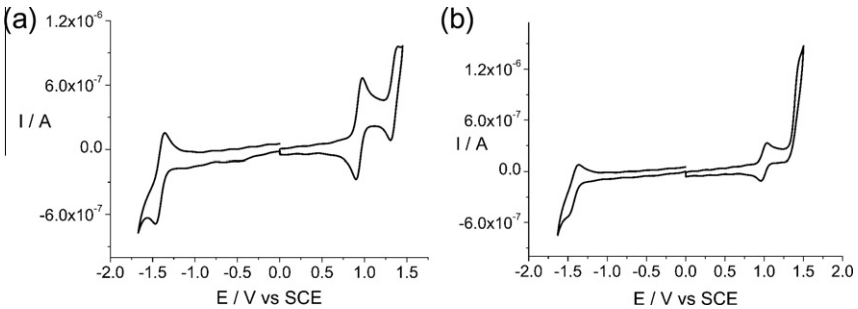

Fig. 3. Cyclic voltammograms of (a) **2c** and (b) **2d**.

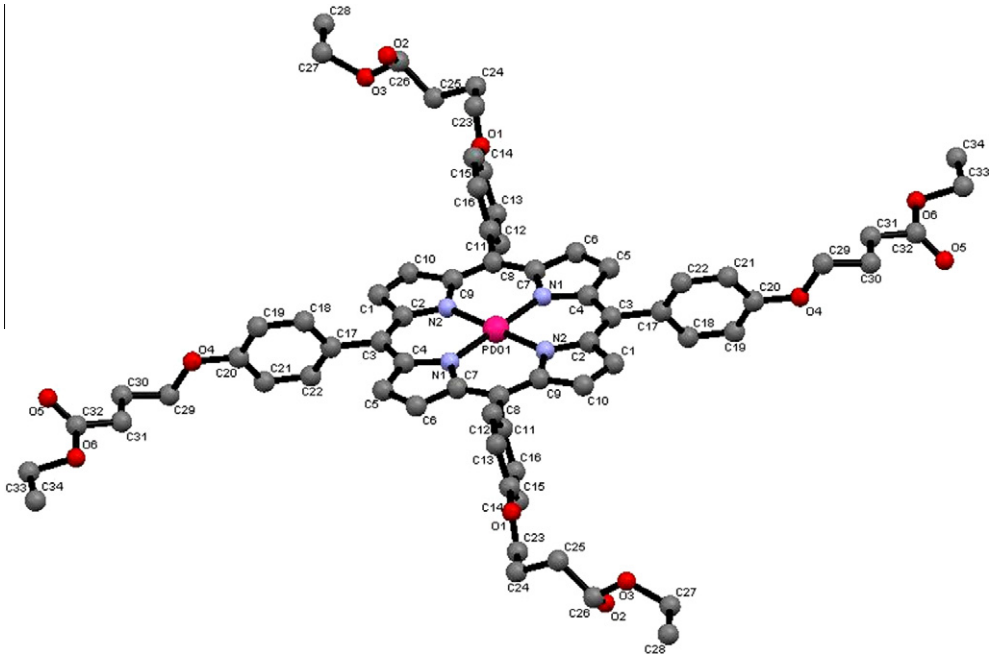

Fig. 4. X-ray structure of complex **2c**. Hydrogen atoms have been omitted for clarity.

mean plane defined by the four nitrogen of the porphyrin core and have planar structure. The packing of the two porphyrins is different (shown in the Supporting info).

3.5. Solar cell measurements

The results of the I/V measurements of the DSSCs sensitized with different complexes are presented in Fig. 6 and summarized in Table 3. The most successful DSSCs are based on Ru-polypyridyl dyes (N3, N719)[39]. For comparison the photovoltaic parameters of the DSSC sensitized with N719 are also presented. The results confirm the activity of the porphyrin complexes in the DSSCs, however the performance of the cells sensitized with porphyrin complexes is low compared to the N719 dye. Furthermore, when compared to the free porphyrin acting as a dye, an addition of the Rh or Pd as a metal complex ion improves the performance of the solar cell. The maximum short circuit current (*Jsc*) reaching 0.49 mA/cm^2 and a maximum open circuit voltage of 0.473 V was

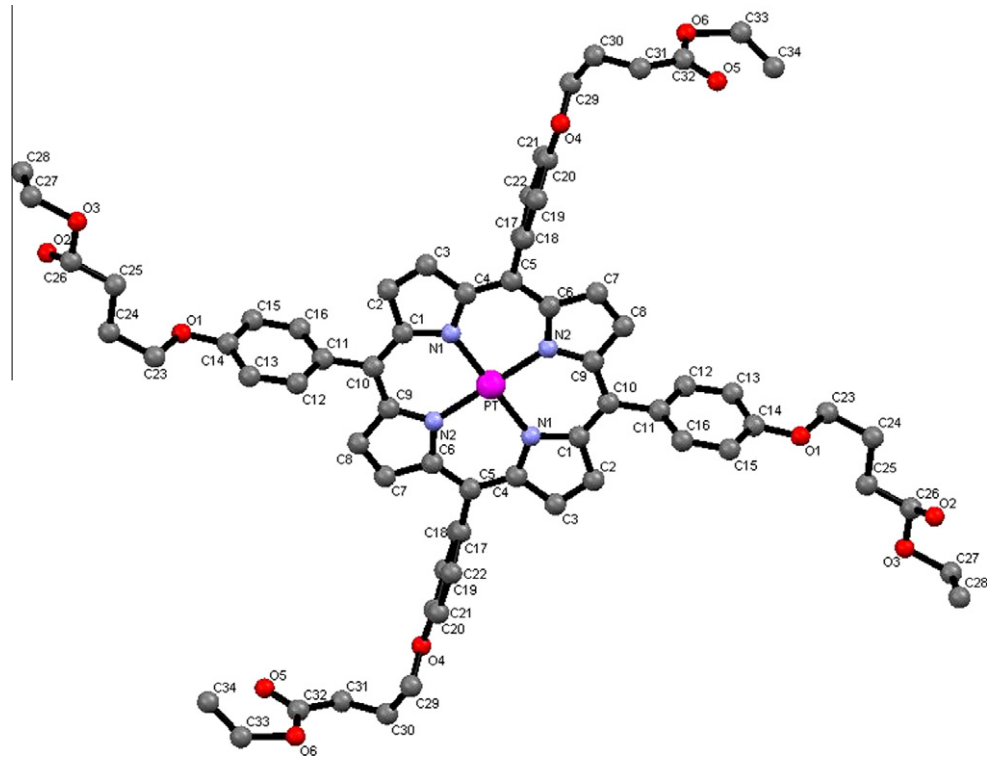

Fig. 5. X-ray structure of complex **2d**. Hydrogen atoms have been omitted for clarity.

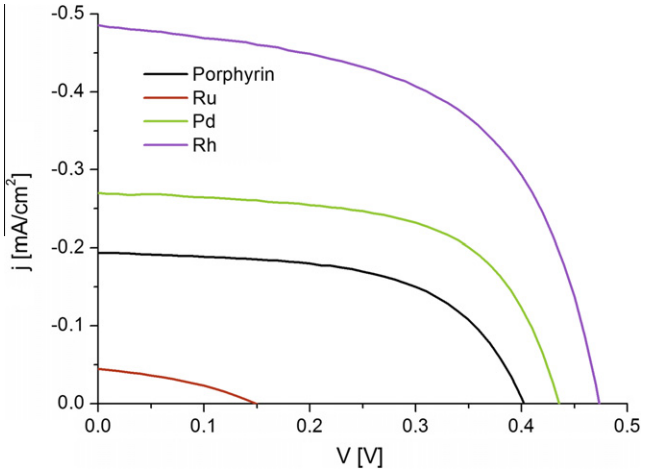

Fig. 6. Current to voltage characteristics of DSSCs sensitized with different porphyrin based dyes.

Table 3
The short circuit current (I_{sc}), fill factor (FF), open circuit voltage (V_{oc}) and conversion efficiency (η) of the DSSCs evaluated under STC (100 mW/cm^2, AM 1.5, 25 °C) for different porphyrin dyes and N719.

Dye	I_{sc} mA/cm2	V_{oc} V	FF %	η %
Porphyrin[a]	0.19	0.402	58	0.045
3a	0.05	0.149	36	0.002
3b	0.49	0.473	56	0.129
3c	0.28	0.435	61	0.075
3d	0.11	0.392	58	0.030
N719	13.80	0.736	64	6.480

[a] Tetra-meso-[4-(3-carboxypropoxy)-phenyl]-porphyrin.

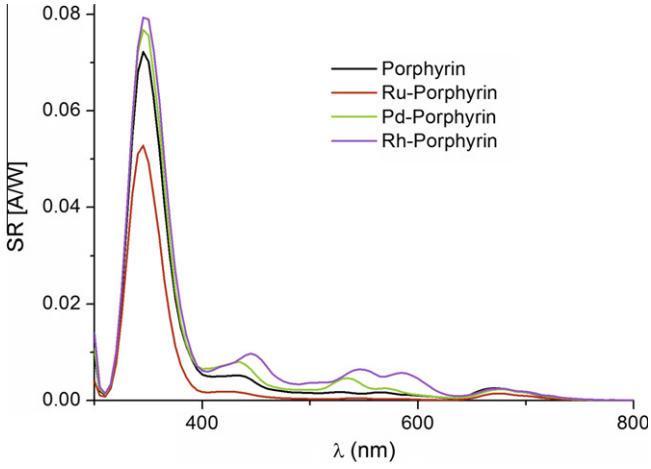

Fig. 7. Spectral response measurements of DSSCs assembled with different porphyrin dyes.

noticed for **3b**. The spectral response (SR) measurements of the DSSCs for different porphyrin complexes are presented in Fig. 7. They are well in agreement with the I/V measurements showing the strongest activity for the complex **3b** in the 400–800 nm spectral range.

Most likely such poor performance of the porphyrin dyes is due to unfavourable energetic positioning of the excited state (LUMO level) of these relatively highly oxidizing dyes in comparison with the N719 dye in the studied TiO2/dye/iodide-triiodide solar cell [40]. An improvement of the DSSC solar cells with the studied porphyrin complexes could be expected if the cell composition would be changed i.e., by choosing a semiconductor with lower potential of the conduction band (e.g. SnO2) and a redox couple with lower potential (e.g., Co2+/Co3+ complexes) [40]. The second option is the development of a novel porphyrin complex with a higher potential of its LUMO level.

4. Conclusions

The synthesis of metallated tetracarboxyporphyrins and their characterization has been presented. The complexes were characterized by UV–Vis, N.M.R. and MALDI-TOF mass spectroscopy. Emmision studies in air-equillibrated solutions indicated that the Pd derivative **2c** shows both phosphorescence (λ_{max} = 710 nm, τ = 752 ns) and fluorescence (λ_{max} = 510 and 616 nm, τ < 1 ns) at 298 K. The Pt derivative **2d** exhibits only the characteristic phosphorescence of platinum porphyrins (λ_{max} = 679 nm, τ = 585 ns) at 298 K. The cyclic voltammograms of complexes **2a**–**d** were measured in CH_2Cl_2 and reversible one-electron oxidations were found in all cases. Pd and Pt derivatives **2c** and **2d** show two oxidations in the range 0.55–0.64 V and 0.95–1.01 versus (Fc/Fc^+). The tetracarboxy derivatives **3a**–**d** was also absorbed on TiO_2 and was tested as sensitizers in DSSCs. The maximum conversion efficiency η = 0.13% gave the Rh-porphyrin complex **3b**. The surface orientation, electronic nature of the porphyrin and electronic communication, all these parameters affects porphyrin's light harvesting ability. In our case, the C_4-alkoxyl chains into the porphyrin ring prevent aggregations but the lack of conjugation at the chains reduces the efficiency of these type of dyes. The use of these noble metals with a different porphyrin structural design (ex. conjugated long chains) might improve their efficiency as dyes in DSSC.

Acknowledgments

Financial support from the European Community's Seventh Framework Programme (FP7) under Grant Agreement No. 229927, project BIOSOLENUTI and Greek Secretariat of Research and Technology (Heraklitos) are gratefully acknowledged.

Appendix A. Supplementary data

CCDC AI631510 contains the supplementary crystallographic data for Pt-tetraester and Pd-tetraester. These data can be obtained free of charge via http://www.ccdc.cam.ac.uk/conts/retrieving.html, or from the Cambridge Crystallographic Data Centre, 12 Union Road, Cambridge CB2 1EZ, UK; fax: (+44) 1223-336-033; or e-mail: deposit@ccdc.cam.ac.uk. Supplementary data associated with this article can be found, in the online version, at http://dx.doi.org/10.1016/j.poly.2012.06.080.

References

[1] B. Choudhury, A.C. Weedon, J.R. Bolton, Langmuir 14 (1998) 6199.
[2] S. Cherian, C.C. Wamser, J. Phys. Chem. B 104 (2000) 3624.
[3] B. Du, C. Stern, P.D. Harvey, Chem. Commun. 47 (2011) 6072.
[4] M. Gervaldo, F. Fungo, E.N. Durantini, J.J. Silber, L. Sereno, L. Otero, J. Phys. Chem. B 109 (2005) 20953.
[5] E. Iengo, G.D. Pantos, J.K.M. Sanders, M. Orlandi, C. Chiorboli, S. Fracasso, F. Scandola, Chem. Sci. 2 (2011) 676.
[6] P.K. Pandley, G. Zheng, in: K.M. Kadish, K.M. Smith, R. Guilard (Eds.), The Porphyrin Handbook, vol. 6, Academic Press, 2000, pp. 157–230.
[7] A. Karmakar, I. Goldberg, CrystEngComm 12 (2010) 4095.
[8] I.D. Kostas, A.G. Coutsolelos, G. Charalambidis, A. Skondra, Tetrahedron Lett. 48 (2007) 6688.
[9] C. Stangel, G. Charalambidis, V. Varda, A.G. Coutsolelos, I.D. Kostas, Eur. J. Inorg. Chem. 2011 (2011) 4709.
[10] M.V. Martinez-Diaz, G. de la Torre, T. Torres, Chem. Commun 46 (2010) 7090.
[11] K. Kalyanasundaram, N. Vlachopoulos, V. Krishnan, A. Monnier, M. Grätzel, J. Phys. Chem. 91 (1987) 2342.

[12] G.K. Boschloo, A. Goossens, J. Phys. Chem. 100 (1996) 19489.
[13] G.A. Crosby, J.N. Demas, J. Phys. Chem. 75 (1971) 991.
[14] C.-W. Lee, H.-P. Lu, C.-M. Lan, Y.-L. Huang, Y.-R. Liang, W.-N. Yen, Y.-C. Liu, Y.-S. Lin, E.W.-G. Diau, C.-Y. Yeh, Chem. Eur. J. 15 (2009) 1403.
[15] A. Yella, H.-W. Lee, H.N. Tsao, C. Yi, A.K. Chandiran, M.K. Nazeeruddin, E.W.-G. Diau, C.-Y. Yeh, S.M. Zakeeruddin, Science 334 (2011) 629.
[16] M.A. Baldo, D.F. O'Brien, Y. You, A. Shoustikov, S. Sibley, M.E. Thompson, S.R. Forrest, Nature 395 (1998) 151.
[17] M. Cocchi, V. Fattori, D. Virgili, C. Sabatini, P. Di Marco, M. Maestri, J. Kalinowski, Appl. Phys. Lett. 84 (2004) 1052.
[18] V.A. Montes, C. Pérez-Bolívar, N. Agarwal, J. Shinar, P. Anzenbacher, J. Am. Chem. Soc. 128 (2006) 12436.
[19] Y. Shao, Y. Yang, Adv. Mater. 17 (2005) 2841.
[20] J.E. Kroeze, T.J. Savenije, J.M. Warman, Adv. Mater. 14 (2002) 1760.
[21] J.E. Kroeze, T.J. Savenije, L.P. Candeias, J.M. Warman, L.D.A. Siebbeles, Sol. Energy Mater. Sol. Cells 85 (2005) 189.
[22] A. Morandeira, I. López-Duarte, M.V. Martínez-Díaz, B. O'Regan, C. Shuttle, N.A. Haji-Zainulabidin, T. Torres, E. Palomares, J.R. Durrant, J. Am. Chem. Soc. 129 (2007) 9250.
[23] G.A. Crosby, J.N. Demas, J. Phys. Chem. B 75 (1971) 991.
[24] J. Van Houten, R.J. Watts, J. Am. Chem. Soc. 98 (1976) 4853.
[25] G.M. Sheldrick, Acta Crystallogr. Sect. A: Cryst. Phys., Diffr., Theor. Gen. Crystallogr. 64 (2008) 112.
[26] M. Hočevar, M. Berginc, M. Topič, U. Opara Krašovec, J. Sol-Gel Sci. Technol. 53 (2010) 647.
[27] U. Opara Krašovec, M. Berginc, M. Hočevar, M. Topič, Sol. Energy Mater. Sol. Cells 93 (2009) 379.
[28] M. Berginc, U. Opara Krašovec, M. Hočevar, M. Topič, Sol. Energy Mater. Sol. Cells 91 (2007) 821.
[29] V. Vasil'ev, I. Blinova, I. Golovina, S. Borisov, J. Appl. Spectrosc. 66 (1999) 583.
[30] S. Drouet, C.O. Paul-Roth, V. Fattori, M. Cocchi, J.A.G. Williams, New J. Chem. 35 (2011) 438.
[31] S. Drouet, C.O. Paul-Roth, G. Simonneaux, Tetrahedron 65 (2009) 2975.
[32] K. Kalyanasundaram, Chem. Phys. Lett. 104 (1984) 357.
[33] M. Ikonen, D. Guez, V. Marvaud, D. Markovitsi, Chem. Phys. Lett. 231 (1994) 93.
[34] D.P. Rillema, J.K. Nagle, L.F. Barringer, T.J. Meyer, J. Am. Chem. Soc. 103 (1981) 56.
[35] K.M. Kadish, K.M. Smith, R. Guilard (Eds.), The Porphyrin Handbook, Academic Press, 2000.
[36] L.M. Mink, M.L. Neitzel, L.M. Bellomy, R.E. Falvo, R.K. Boggess, B.T. Trainum, P. Yeaman, Polyhedron 16 (1997) 2809.
[37] B.B. Wayland, A.R. Newman, Inorg. Chem. 20 (1981) 3093.
[38] X.H. Mu, K.M. Kadish, Langmuir 6 (1990) 51.
[39] A. Hagfeldt, G. Boschloo, L. Sun, L. Kloo, H. Pettersson, Chem. Rev. 110 (2010) 6595.
[40] G.F. Moore, S.J. Konzenzy, H. Song, R.L. Milot, J.D. Blakemore, M.L. Lee, V.S. Batista, C.A. Schmuttenmaer, R.H. Crabtree, G.W. Brudvig, J. Phys. Chem. C 116 (2012) 4892.